Proceedings of the ASME 2018 Internal Combustion Fall Technical Conference
ICEF2018
November 4-7, 2018, San Diego, CA, USA

DRAFT - ICEF2018-9567

DESIGN OF AN ADVANCED AIR PATH TEST STAND FOR STEADY AND TRANSIENT EVALUATION

R Vijayakumar
Powertrain and Vehicle Research Centre
University of Bath,
Bath, BA2 7AY, UK

R Burke
Powertrain and Vehicle Research Centre
University of Bath,
Bath, BA2 7AY, UK

Y Liu
Powertrain and Vehicle Research Centre
University of Bath,
Bath, BA2 7AY, UK

JWG Turner
Powertrain and Vehicle Research Centre
University of Bath,
Bath, BA2 7AY, UK

ABSTRACT

Different air systems such as turbochargers (TC), hybrid boosting, turbo compounding and exhaust gas recirculation (EGR) are increasingly used to improve the thermal efficiency of internal combustion engines (ICE). One dimensional (1D) gas dynamic codes supports their development and integration by modelling the engine and air systems and reducing testing time. However, this approach currently relies on steady flow characteristic maps which are inaccurate for simulating transient engine conditions. This is a key weakness of using gas-stand measured maps in engine simulations. Performing TC mapping on an engine would in principle solve this problem, however engine-based mapping is limited by the engine operating range and on these facilities, high-precision measurements are challenging.

In addition, simple turbocharging can no longer be constrained to an individual TC supplying boost air to an engine. Instead, modern downsized engines require air-path system making use of multiple components including TCs, mechanical superchargers, electrically driven compressors (EDCs), EGR paths and control valves. Thus studying multiple air systems requires an experimental test facility to understand how they work in synergy. This is also useful in developing empirical models to minimize test time. Therefore the aim of this paper is to present a novel experimental facility that is flexibly designed for evaluating air systems individually and also at the system level representing a complicated air path both in steady and transient condition.

The advanced test facility is built around a 2.2 l diesel engine to test the above air systems which can isolate the thermal and load transients from engine pulsating flows. Removing the flow pulsation allows study of the system characteristics in a steady state. Several examples of component and system level tests including a two-stage air path comprising of a VGT (variable geometry turbine) TC and a 48V EDC with typical operating condition (provided by 1D modeling) are discussed.

KEYWORDS

Engine gas stand, Compressor characteristics, Turbine characteristics, Transient characteristics, Electrically driven compressor, LP EGR, HP EGR, turbocharging

NOMENCLATURE

Symbols

$\dot{m}_a$	Air mass flow rate
γ_{3-4}	Average ratio of specific heat across turbine
C_{pa}	Average specific heat of air across the compressor
C_{pe}	Average exhaust gas specific heat across the turbine
$\dot{m}_e$	Exhaust gas mass flow rate
PR_{3-4}	Pressure ratio across the turbine
T_{01}	Total compressor inlet temperature
T_{02}	Total compressor outlet temperature
T_{03}	Total turbine inlet temperature
η_t	Turbine efficiency

Abbreviations

Air fuel ratio	AFR
Carbon dioxide	CO2
Charge air cooler	CAC
Combustion air handling unit	CAHU
Compressor back pressure valve	CBPV
Computational fluid dynamic	CFD
Controller Area Network	CAN

Divided exhaust period	DEP
Electrically driven compressor	EDC
Engine Gas Stand	EGS
Emergency stop	e-stop
Exhaust gas recirculation	EGR
Field-programmable gate array	FPGA
Gas stand (Conventional)	GS
High-pressure EGR	HP-EGR
Internal combustion engines	ICE
Mass flow parameter	MFP
Low-Pressure EGR	LP-EGR
Nitrogen oxide	NOx
One dimensional	1D
Pressure ratio	PR
Total-to-Static	T-S
Turbine inlet temperature	TIT
Turbocharger	TC
Variable geometry turbine	VGT
Variable valve actuation	VVA

1. INTRODUCTION

Legislation that demands reduction of carbon dioxide (CO_2) emissions and fuel consumption in the automotive segment is ever increasing. Consumer choice of the ICE is still most common irrespective of the arrival of alternative propulsion system such as fuel cells or full electric vehicles. This is due to several drawbacks of these such as high cost, low durability, large system size and weight, slower dynamics, etc., [1], and in the case of hydrogen based fuel cells, poor hydrogen infrastructure and safety [2] which limits their use. ICEs are the primary source of power production in most plug-in hybrids [3]. Thus, the ICE will continue to be an important source of motive power for the foreseeable future [4]. Adequate improvement in powertrain systems using efficient technologies will help to address and meet the future legislation [5]. The efficiency of the ICE has been increased considerably greater than 50% by recovering exhaust gas energy using turbochargers and waste heat recovery systems in combination with downsizing and down speeding [6].. However the poor transient response and poor low speed engine torque due to lower boost pressures are some of the limitations to this technology. Recently EDCs have been introduced to produce low-speed boost pressure to improve engine torque and acceleration giving excellent transient response [7]. As the engine efficiency improves with engine load generally, the electric power consumption for driving the supercharger is balanced by load increase [8]. Also by pumping some exhaust gases back into the cylinder with EGR, nitrogen oxide (NO_x) emissions are reduced. Thus different air systems can help improve engine thermal efficiency and/or engine power (in various configurations) [9] [10] [11] [12]. To meet emissions and fuel consumption targets much more complex boosting systems are needed going forward. This requires accurate models and the experimental validation of such systems. Thus a flexible facility to test the system level integration is of paramount importance.

The above mentioned technologies are supported by system integration with the support of one dimensional (1D) gas dynamic modeling simulating engine and air systems performance. As the 1D modeling tools speed up the engine development process they are popular in automotive research. Generally, the 1D modeling tools use steady state derived TC maps obtained from conventional gas stands (GS) with hot air at 600°C at the turbine inlet. Such a facility typically includes the capability to measure the TC speed, pressure, temperature and mass flow rate across turbine and compressor. Corrections are given to the measured mass flow and speed to account for any difference in conditions (temperature and pressure).

The flow on an engine is very different to the steady flow conditions seen on conventional GSs due to the pulsating flow caused by valves and changes in engine operating conditions. The 1D models use approaches that adopt the classical quasi-steady assumption using the turbine map as a look up table at each instance of time during the exhaust pulse thus predicting instantaneous behavior based on the steady flow mapping data [13] [14]. This is a key weakness of using gas-stand measured maps in engine simulations. Performing TC mapping on an engine would in principle solve this problem, however engine-based mapping is limited by the engine operating range and on these facilities, high-precision measurements are challenging.

In addition, turbocharging can no longer be constrained to an individual TC supplying boost air to an engine. Instead, modern downsized engines require air-path systems making use of multiple components including TCs, mechanical superchargers, EDCs, EGR paths and control valves. Thus, the aim of this work is to create an advanced test facility suitable for precisely analyzing and isolating the behavior of future air path configurations operating under real engine conditions. The paper presents an approach to build a steady flow engine based gas stand test facility with minimal support from 1D gas-dynamic modeling. Test results including turbine, compressor characteristics and those of an EDC are presented. Also, of particular note is the ability of the facility to test the performance of multiple air systems (system level tests). An example case of a 2-stage boosting system comparing the effect of achieving target boost pressure by varying the vane angle of a VGT versus the power required for an EDC is also shown.

This work was conducted as part of the EU Commission funded THOMSON Project (http://www.thomson-project.eu/, grant number 724037). The project aims to increase the market penetration of 48V hybrid vehicles.

2. BACKGROUND

Typically, in simulation the steady flow characteristic turbine and compressor maps are fed into 1D modeling tools that use it as a look up table in a quasi-steady process (notwithstanding that the flow is unsteady in an engine). Due to the limitation in the turbine data obtained (limited by compressor surge and choke) extrapolation methods are adopted in 1D modeling leading to possible inaccuracies [15]. Also the pulsating flow in an ICE involves complex flow and heat transfer which necessitates facilities with pulsating flow capability. A number of attempts have been made to recreate engine-like pulsations within a TC gas-stand environment. A rotary valve of specific designs varied the pulse shape and amplitude while a variable speed motor determined the pulse frequency [16]. A similar mechanism but with a different number of slots on the swappable rotary disk determined the number of pulses per cycle [17]. Pulsations have also been generated by counter rotating plates but at lower temperature [18]. The pulse profile does not resemble that from an engine due to the nature of the mechanism used. In another design, a cold test facility with a cylinder head and valves from an actual engine using a variable valve actuation (VVA) generated closer-to-realistic engine pulses [19]. Finally, an advanced version of cylinder head pulsation generator that can handle hot gas with an active valve train and an integrated exhaust manifold produced hot pulses closer to modern ICE [20].

Another limitation of the facilities described above is the difficulty in replicating engine transient events on the GS. For example, a a step-change in load cannot be performed on the GS due to the limitation of electrical heaters. [21]. Some researchers have used external boost systems for the engine with a pulse attenuator to dampen flow pulsations at the turbine inlet. [22] [23]. These facilities measured the steady flow TC performance in general although pulsating flow and transient measurement were made of measurable parameters (for 1D modeling). Thus a facility that is functionally between a GS and engine is extremely useful. The facility discussed in this paper is in principle similar to the one described in [22] and [23]. However, a primary difference is the ability to combine multiple air systems which to the authors' knowledge, no other work has considered or attempted.

The facility discussed here was upgraded from a previous version which had the turbine mounted directly on the exhaust manifold seeing pulsating flow at the turbine inlet. The compressor was isolated from the engine inlet to work against a compressor back pressure valve (CBPV). The setup was used to observe certain unsteady flow TC behaviors [24][25], and used to improve 1D modeling accuracies [26] [27] and identify the effect of modifying the positions of intercooler on a 2 stage boosting system [28]. Although similar engine gas stand (EGS) rigs are in operation globally, there are a few important features to note here that allows the study of complex air handling systems. The facility discussed in this paper is the next generation of the facility discussed in reference [24] to [28] which had difficulties measuring turbine-side flow.

The approach adopted in this paper could be summarized as trying to improve the representativeness of gas-stand testing. The test facility discussed in this paper can produce steady flows as in a conventional GS to characterize the turbine and compressors under steady flow conditions. It also has the ability to produce actual engine-like pulsations and transient events. The experimental setup also allows to utilize the exhaust gas from the engine to study the influence of high-pressure EGR (HP EGR), low-pressure EGR (LP EGR) and mid-route EGR together with a 2-stage boosting system involving a first stage TC compressor and a second stage EDC. Thus multiple air system configurations could be studied experimentally. These are described in detail throughout the paper.

3. DESCRIPTION OF THE TEST FACILITY

3.1 REQUIREMENTS OF THE TEST FACILITY

A steady flow facility is important for steady state characterisation of air systems. However, the ability to produce real-time engine pulses and engine-like transients are equally important for the unsteady and transient characterisation of TCs. This is particularly useful in studying and improving the engine-air system interaction leading to an efficient component design and control strategies. This dataset is valuable and would be useful to validate the 1D and 3D Computational Fluid Dynamic (CFD) simulations that are used in designing TCs. Also a facility to test the impact of LP EGR and HP EGR in combination with a single-stage and multi-stage boosting system is very useful. This could be for multiple reasons:

i. It would help improve the process building and validate 1D models
ii. System-level studies for a combination of above mentioned air system and also on specific aspects could be done without requiring the prototype engine. For example: investigations into positioning the charger air cooler before or after the second stage boosting system could be made.
iii. Control strategies could be effectively studied. For example: achieving target boost either with higher turbine power by closing the VGT or with EDC power
iv. Such a facility could help design better air paths
v. The transient performance at the system level could be tested without having the actual engine. For example: Transient system response from transporting EGR.
vi. Also, the exhaust gas from the engine in the facility can be used to tell the effect of exhaust gas heat loss on the catalytic light off time. This is a very important aspect [29] while taking measures to minimise the light-off time [30][31], especially when designing and testing TCs to minimise exhaust gas heat loss to reduce the catalyst light-off period.
vii. Finally, it can also be used to understand complex exhaust systems such as turbo-discharging [32], divided exhaust period (DEP) [33] etc. and energy availability, for example:

how valve timings or lift profiles affect charging system performance.

3.2 FUNCTIONAL SPECIFICATION OF THE TEST FACILITY

The advanced air path test facility is required to have the following capabilities:

i. Produce gas flow rates covering a similar steady-state mapping region of turbine, compressor, and EDC to conventional steady flow GSs. The operating ranges are required for turbine and compressor are specified in **Table 1**.

Table 1: Maximum steady flow specification requirements of advanced air path test facility

	Turbine	Compressor	EDC
Maximum mass flow (Kg/h)	600	600	600
Inlet pressure (bar)	Up to 4bar	~1bar	1-2
Outlet pressure (bar)	1-1.3	1-3bar	1-3
Maximum Inlet temperature (°C)	800	30	100
Maximum outlet temperature (°C)	600	250	250

ii. Allow independent control of turbine inlet temperature (TIT) and mass flow
iii. Be able to test a turbine and compressor under steady and engine load-like transient conditions (engine warm-up or engine load change) with and without pulsating flows
iv. Be able to test a full air path system with different air path routings including the recreation of different EGR paths (low- and high-pressure).
v. Provide 48V electric power up to 5kW for EDC testing
vi. Provide independent conditioning of lubricating oil and cooling water for the air path components.
vii. Incorporate adequate safety systems in line with the prototype nature of the test facility

This covers the important aspects involved in this research.

3.3 LAYOUT OF ENGINE GAS STAND TEST FACILITY

The schematic of the EGS test facility is shown in **Figure 1**. For the sake of understanding the test facility can be classified into three parts: the boost rig, the engine and the gas stand as shown in **Figure 1**. Stainless steel pipe work connects the above three parts as explained in this section. **Figure 2** shows the picture of the experimental setup. Same numbers are given for parts in **Figure 1**and **Figure 2** to help understand their location in reference to the schematic. It is important to note that the tested air path could be any complex air path. As an example case, the air path from the Thomson project is discussed in this paper. Compressed air up to a maximum pressure of 8 bar and 0.7 kg/s mass flow rate is fed from external compressors and an air drier that removes the moisture (not shown in **Figure 1**and **Figure 2**). A ball valve with a Kinetrol actuator controls the air pressure and mass flow rate going into the boost rig also referred to as a combustion air handling unit (CAHU). The boost rig can independently control the air temperature and pressure and flow rate of air going into the engine. Air becomes an intrinsic part of the exhaust gas after undergoing combustion with the fuel. The engine speed and load are varied to keep a steady exhaust gas temperature (usually 550°C) at the turbine inlet. Also, the flow through the boost rig could be adjusted to get the same effect depending on the flow requirement of the test point.

Hot exhaust gas from the engine (2 in **Figure 1**and **Figure 2**) then passes through a three-way pulse attenuator (3 in (2 in **Figure 1**and **Figure 2**)which dampens the pressure pulsation significantly to near steady flow levels. The three-way tank can route the gas to either turbine inlet or HP EGR path or both. Exhaust gas then passes through the measuring sections at the turbine inlet (4 in **Figure 1**and **Figure 2**) powering the TC and pass through to the outlet measuring section (6 in **Figure 1**and **Figure 2**). The exhaust gas can either be sent through the LP EGR path (5 in **Figure 1**and **Figure 2**) to the TC compressor inlet or could be directly vented through the extract system (7 in **Figure 1**and **Figure 2**). The settling tank could be bypassed to test the unsteady flow and transient effects on the component and system level performance.

The exhaust gas from the HP EGR path (5 in **Figure 1**and **Figure 2**) could be routed in three different ways: mid route1 (connected to outlet of CAC), mid route2 (connected to inlet of CAC) and HP EGR (outlet of EDC) to observe different physical and thermal aspects of the TC compressor and EDC. There is a T-piece in the HP EGR route that is connected to a burst disc made of Inconel 625. This protects the system components from any pressure surges above 6.5 barA (with +/- 5% tolerance rated at 600° C) by bursting open and venting the pressure to the extract system (7 in **Figure 1**and **Figure 2**).

On the other side, air is sucked in by the TC compressor and goes via an ABB Sensyflow mass flow meter (5 in **Figure 1**and **Figure 2**). It can either go through the TC compressor directly or be combined with the LP EGR (if used) before going through the TC compressor. On a single-stage boosting setup, a back pressure gate valve controls the mass flow through the compressor or the compressor outlet pressure. A 5kW EDC (5 in **Figure 1**and **Figure 2**) powered by a programmable DC supply forms the important part of the second-stage boosting system. On a 2-stage boosting setup, the air from the TC compressor goes through a charge air cooler (CAC) (5 in **Figure 1**and **Figure 2**) and subsequently through the EDC and the back pressure gate valve.

A bespoke temperature-controlled oil system regulates lubricating oil flow through the TC. A temperature-controlled water system (Regloplas 90 smart, not shown) was used to regulate and to cool the EDC. Water supplied from a local pond

cools down both oil and water to the set temperature. The specification and further details of the standalone units are provided in **section 3.5.4**. The sensors used, position on the rig, accuracy, resolution and measurement frequency are specified in **Error! Reference source not found.**. In case of an emergency, the emergency stop (e-stop) button on the Sierra CP winged keyboard safely stops the fuel pump, dynamometer, boost rig, oil conditioning system and the coolant units thus stopping the engine and standalone rigs. The 3-phase digital switches are controlled from Sierra CP. A high-pressure water sprinkler system is kept ready to suppress fire, in the unlikely event that this happens.

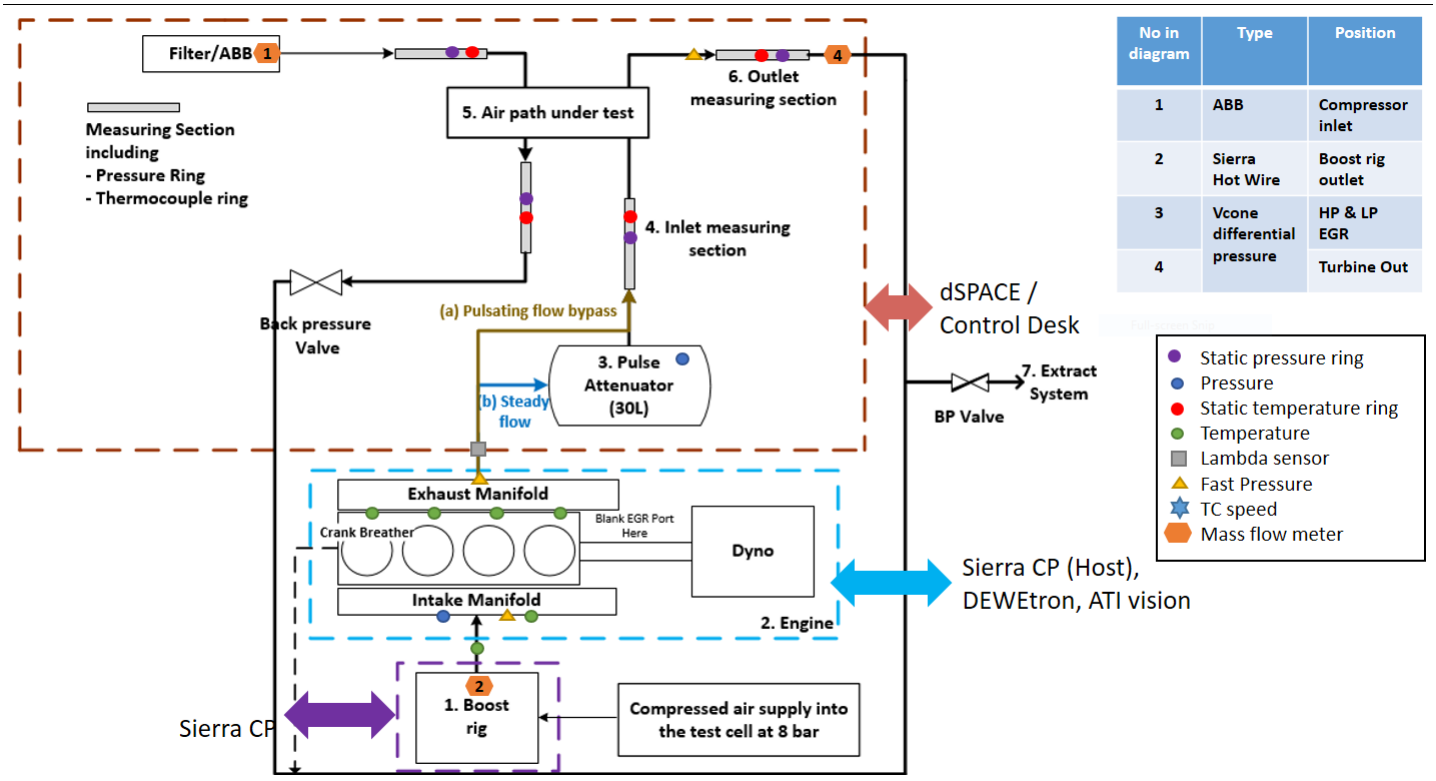

Figure 1: Schematic of the EGS experimental setup

Table 2: Sensor location, type, make, accuracy, and measurement frequency

Position/ Purpose of the sensor	Sensor type and Manufacturer/Model name	Accuracy / Resolution	Dewetron (10kHz) / CP (40 Hz)
TC speed	Eddy current – Micron Epsilon DZ135 sensor	FSO resolution of ±0.22%	Both
Engine outlet and Turbine outlet static pressure	Water cooled Piezo-Resistive – Kistler sensors 4049B10DS1 and 4049A5s respectively	± 0.08% linearity of full scale output	Dewetron
Compressor inlet and outlet static pressure	Piezo resistive silicon elementPXM419-3.5BAV and PXM419-002BGV	±0.08% FSO	CP
Compressor inlet air mass flow rate	ABB Sensyflow FMT700-P (hot-film anemometer)	< ± 1 % of measured value	CP
Average turbine/compressor/EDC inlet and outlet temperature	K Type thermocouples - TC Direct Pt100 (Precision)	± (0.15+0.002*t)	CP

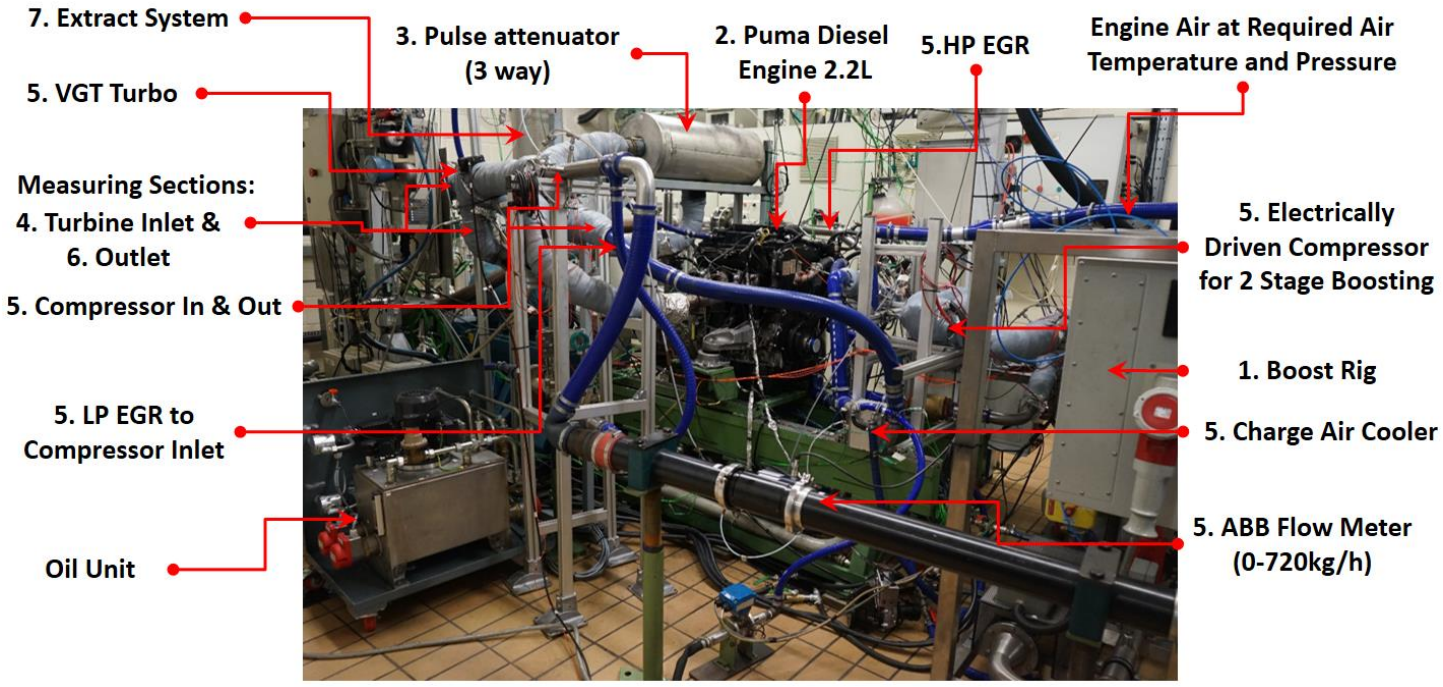

Figure 2: New air path test facility

3.4 INITIAL ONE-DIMENSIONAL MODELING TO SPECIFY THE SETTLING TANK

The first step is to use 1D modelling to suggest design parameters of the pulse attenuator. Section 3.4 describes this in detail. The second step is to manufacture it and also procure secondary components (like oil and coolant conditioning system) and assemble the pipe work to get it test ready. This is followed by component level, system level and transient tests based on the requirements. The obtained data are used for different purposes as described in section 3.1.

Due to the limitation in the availability, cost and accuracy of certain instruments it has traditionally been difficult to measure the instantaneous turbine flow with pulsating conditions. The unsteady flow produces an operating profile (of the turbine and compressor) created by the varying TC speed and boundary conditions as opposed to a single operating point at constant speed obtained from the GS. Hence for the turbine especially a portion of the typical operating profile tends to be outside the region of these steady-state data maps. For this reason it is advantageous to be able to remove the pulsations from the engine exhaust flow and this is the motivation behind the pulse attenuator. With this installation, the test rig can still provide thermally transient boundary conditions such as those seen on engine, however the turbine flow rate can be measured using conventional mass flow meters.

A settling tank was specified based on the 1D gas dynamic modeling work done with an already validated 2.2 l engine model (discussed in [27]). The 1D modeling involved studying the flow dampening effect for six different cylinder volumes as shown in **Figure 3:** . A 30 litre tank volume was chosen as it dampened the flow pulsations significantly, producing an almost steady flow at the tank outlet. A 3D model of the settling tank assembly used in the tests is shown in **Error! Reference source not found.Figure 4**. The size of the settling tank would also suit the test cell arrangement and hence the manufacturing was outsourced. The attenuation tank is insulated to maintain temperature with a high temperature material which is supported by an external cladding. The installation in the test facility is shown in**Figure 2**. The next section discuss the hardware used in the EGS test facility that is suitable to measure the steady and transient TC performance. Also, the measurement and control systems used in capturing data and the details of the hardware controls are discussed in sections 3.6 and 3.7 respectively.

3.5 EGS HARDWARE AND CONTROL SYSTEM

A photo of a fully operational test rig with the important components is shown in **Figure 2**. The important constituents of the rig, their purpose, specification and usage are discussed in this section.

3.5.1 2.2 L DIESEL ENGINE

The rig is based around a diesel engine rather than a gasoline engine as this provides the possibility to adjust fuel flow independently of air flow and therefore control exhaust gas temperature and air flow independently. The engine at the centre of the advanced test facility is a 2.2 l diesel engine. The engine is in series production and therefore a robust platform. The series production engine is turbocharged and uses common rail fuel

injection. By selecting an engine with larger displacement it can deliver the required range of mass flows and ensures an engine-independent metric of the TC performance. Some overall engine characteristics are listed in **Table 3** and the test setup with the engine is shown in **Figure 2Error! Reference source not found.**.

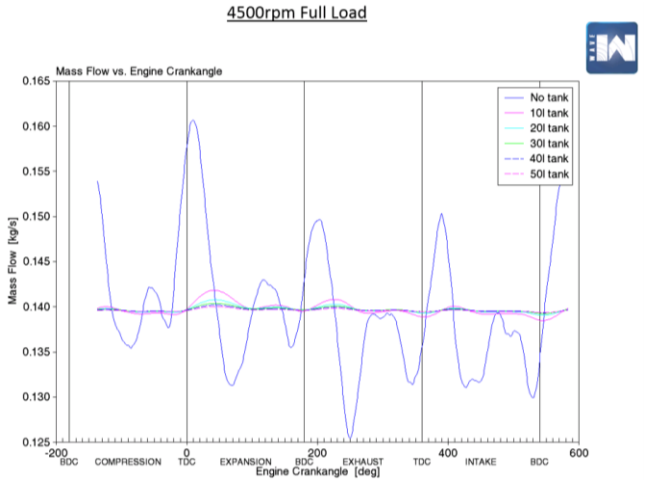

Figure 3: 1D simulation showing the effect of tank volumes on the mass flow pulsation at the tank outlet

Table 3: Summary specifications of the 2.2 l diesel engine used in the test facility

Parameter	Value
Peak exhaust gas mass flow	500kg/hr
Max exhaust gas temperature from engine	850°C
Exhaust gas temperature limit due to operating range of the settling tank	650°C

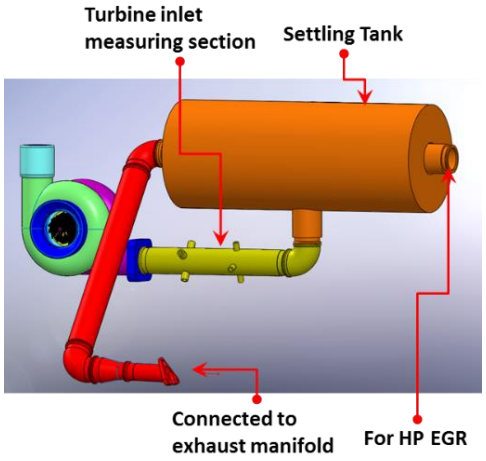

Figure 4: 3D model of the settling tank connected to exhaust pipework and inlet measuring section

3.5.2 EXTERNAL BOOST RIG (CAHU)

The external boost rig provides boost air to the diesel engine. The boost facility is supplied by an industrial screw compressor that provides up to 1000kg/h or dry and cooled air at 8bar pressure. The boost rig is located between this supply and the engine intake manifold and uses a series of control valves, heaters and coolers to control the delivery pressure and temperature of air to the engine. The rig is designed to respond approximately 10 times faster than a TC allowing for engine-like transients. The operating range of the boost rig is summarised in **Table 4**. The reader is advised to refer [34] for a comprehensive description.

Table 4: Summary specifications of the boost rig

Parameter	Value
Air deliver pressure	1.2-6bar
Pressure control accuracy	+/-0.5%
Maximum flow rate	700kg/hr
Maximum temperature	60°C
Minimum Temperature	20°C
Temperature accuracy	+/-1°C

3.5.3 TURBOCHARGER MEASUREMENT UNIT

The turbine inlet and outlet flanges are mounted at the end of a measuring section which is connected to the settling tank as shown in **Figure 4**. Hot exhaust gas at typical engine conditions powers the turbine which in turn powers the compressor. The compressor inlet stub and outlet flange are also connected to two measuring sections. Each of the four measurement sections has four ports for thermocouples or PRTs at 90° to each other. Four radial tappings at 45° angle to the temperature tappings were connected by a manomeric ring to measure the average static pressure. This eliminates the difference in pressure in the pipe across the measuring section. . The number of thermocouples/PRTs and their lengths inside the measuring sections are specified in **Figure 5** and **Table 5.**

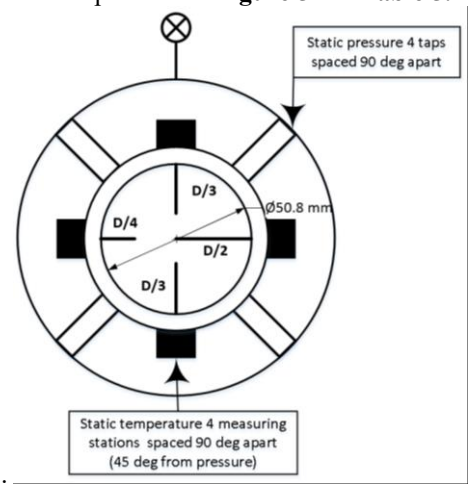

Figure 5: Thermocouple lengths and pressure ring orientation in the compressor outlet and turbine and inlet and outlet measuring sections

Table 5: Specification of pressure and temperature measurement using test sections

Measurement sections location	Static pressure type	No of static temperature ports	Lengths of thermocouples/PRTs
Compressor and EDC inlet	Static pressure ring with 4 ports spaced at 90° interval to measure the average static pressure and 45° from temperature ports	2	1/3 diameter of the tube at 180° relative to each other and perpendicular to tube walls
Turbine inlet		4	1/3 diameter at 0° and 180°, 1/2 diameter at 90° and 1/4 diameter at 270°
Turbine outlet		4	
Compressor and EDC outlet		4	

3.5.4 OTHER MECHANICAL AND HYDRAULIC SYSTEMS

Besides the mechanical systems described above, the rig includes a flexible EGR system providing HP, LP and mid-route EGR paths with aftermarket components from the passenger car segment. The EGR valves are controlled from dSPACE with a 0-5V analogue voltage signal proportional to the opening position. The engine coolant flow is extended via coolant manifolds (feed and return) as shown **Figure 6** and used as a source of cooling for the EGR valves and heat exchangers and are conditioned to approximately 90°C.

Cooling systems are used to maintain the temperature of engine components, EDC, EGR valve and EGR heat exchanger. Overall cooling is provided by a central water cooling supply for the building facilities. A proportional Kinetrol valve (electro-pneumatic servo valve) is used to maintain the engine components within a specific temperature, and this is controlled through the Sierra CP software via a PID loop to a set point (temperature). A Regloplas P140 smart coolant system with user specified temperature regulates the TCs and EDCs operating temperatures. It uses the central pond water supply to maintain the coolant supply temperature and as top up for the cooling water for the water lost in evaporation. The EGR valves and the EGR heat exchangers are cooled by extending the engine coolant pipe and a manifold (as shown in **Figure 6**).

The lubrication oil for the TC bearings is supplied by a standalone unit. The position of it within the test cell is shown in**Figure 2**. A screw pump sends oil from a 7 gallon mild steel tank fitted with three 1kW heaters and can supply up to 10 l/m. The oil is pumped from the tank via a plate water cooler, an in-line filter with a bypass and an electrical clogging indicator. The oil flow can be supplied to two branches each of which incorporates a flow control valve and flow meter. The water-side cooler includes a solenoid-operated valve to regulate water flow through the cooler. This valve splits the main line into two feeds in order to obtain individually adjustable output in each leg. The main pressure lines also include a temperature indicator which works in conjunction with the cooler and the heater fitted in the tank to maintain the required temperature. The tank also includes a visual level gauge, a filler/breather, a drain valve and the oil return. The control system is housed in an enclosure and comprises of a Danfoss +1 controller. The outside of the enclosure incorporates an e-stop and the motor start/stop buttons. Inside of the enclosure the controller, switch gear for heaters, motor and cooler solenoid valve and a 24V DC supply is housed. The control system monitors and maintains the oil temperature by switching the heater and cooler as required.

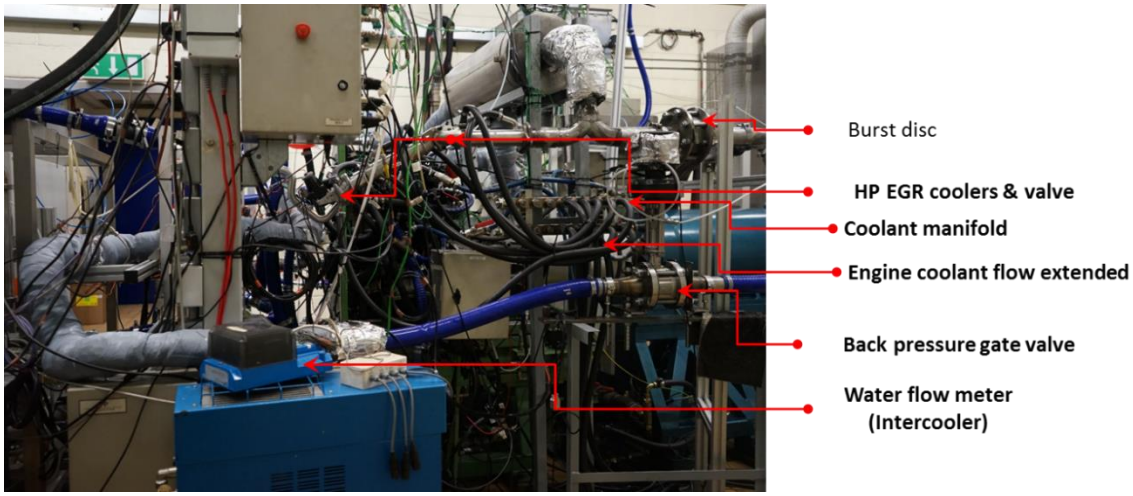

Figure 6: HP EGR cooler and pipework to be connected to HP EGR valve and silicone hoses

3.6 MEASUREMENT AND DATA PROCESSING SYSTEM

For acquiring data in the steady and unsteady flow experiments specific data acquisition software is used. A schematic of the parameters recorded and the software used are shown in **Figure 7**. The steady flow data required for mapping the turbine and compressors will be recorded at low frequency (40 Hz) using proprietary software by Sierra CP. The pressure, temperature, mass flow rate and TC speed sensor measurements are made in the software with pre-calibrated physical channels. Also, the control of engine speed and load and the CBPV (used to vary the flow rate) are done through this.

High frequency measurements are made using proprietary hardware and software from Dewetron. For example, the compressor surge characteristic study requires high frequency pressure measurement at the compressor outlet. Hence it will be recorded by the Dewetron equipment. Also, experiments involving any pulsating flows and engine transients involve fast changing conditions and necessitates fast data acquisition. For example, instantaneous exhaust pressure pulsations and TC speed data are required in the above experiments and hence will be connected to the Dewetron equipment. This has the capability to measure data up to 200 kHz but is usually limited by the response time of the sensors. ATI vision is a robust software solution that can acquire the ECU data and modify closed loop controls. In this work it will be used to control and regulate the exhaust gas temperature at the turbine inlet. This is usually achieved by changing the amount of fuel injected to the engine.

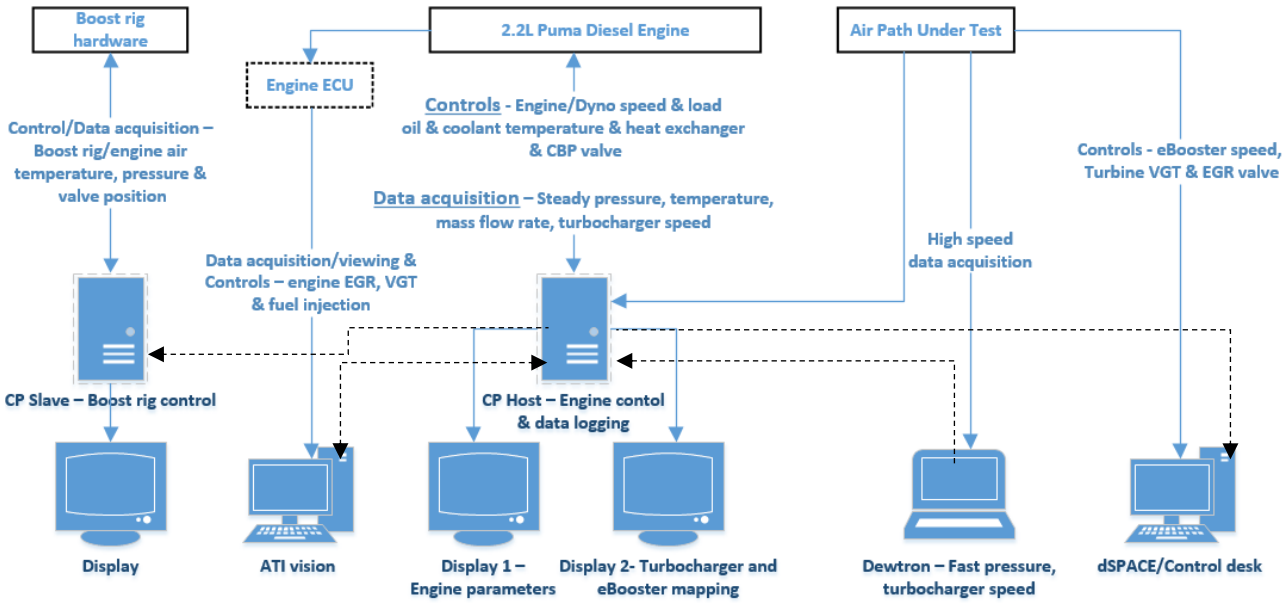

Figure 7: Communication diagram of the test facility

3.7 CONTROL SYSTEMS

To operate the test facility, the user controls the engine/dyno speed and load, EDC speed, turbine VGT position, certain valves and other important parameters. A schematic of the control software and the parameters controlled are shown in **Figure 7**. A central CP Engineering system acts as a host system and sends commands to a CP slave controlling the boost facility. Besides this, the ATI vision system monitors and adjusts ECU parameters manually (if required), and a dSPACE system controls the prototype air path (described in section 4.1). Most of the controls related to the gas stand are controlled using dSPACE, a robust and compact proprietary hardware that includes a comprehensive I/O interface including Controller Area Network (CAN), Ethernet etc. The CAN interface allows two-way communication and control between the microcontrollers and the devices without a host computer. The Simulink-based field-programmable gate array (FPGA) offers programming features to achieve the required functionality. The embedded PC (Windows based) and the Control Desk (graphical user interface) are easily programmable and are made to suit the project requirement. Various I/O interfaces allow the control of different hardware as summarised in **Table 6**.The EDC speed is controlled between 0 to 70000 rpm via a CAN signal from dSPACE. The EDC requires 48V and a 5kW power DC power which is supplied by a Magna Power programmable DC supply (TDS50-300/415 + LXI). It can supply up to 50 V dc, 300A dc and 15kW. The input power required is a 3-phase supply, 374-457V ac and 30 A ac at 50-400 Hz. EGR valves (poppet type) are controlled with a 0 to 5V analogue signal from dSPACE. VGT vane angle is regulated by an aftermarket regulator (VNTT pro). The change in VGT angle also brings a change in pressure ratio (PR) across the turbine. The CBPV regulates the back pressure from the TC compressor or the EDC (depending on the configuration), and is

controlled by a 0 to 10V analogue signal from Sierra CP. This controls the flow and PR across the TC compressor or EDC .

Table 6: Control parameters and specification

Control parameter	Variable	Communication type	Signal Range	Range	Power Supply	Software
EDC speed control	EDC speed	CAN	-	0 to 70000 rpm	48V	dSPACE
VGT vane angle control	Turbine vane angle and PR	Analogue voltage	0-5 V	0 to 100%		
HP and LP EGR valve lift	EGR %	Analogue voltage				
CBP valve	Compressor PR	Analogue voltage	0-10 V			Sierra CP

3.8 SENSORS

Different fluid types are involved in operating an EGS for specific purposes and their flow rate have to be measured precisely. The types of fluids used, purpose, location in the test rig, flow meter and measurement principles are described in **Table 7**.

Air flow through the compressor is measured using an ABB hot wire flow meter at the compressor inlet; this will be corrected later based on the inlet total temperature and total pressure measured. The air flow via the boost rig is measured using a Sierra hot wire flow meter before it enters the engine. The exhaust gas flow through the turbine and the EGR path are measured using Vcone differential pressure flow meter. The oil flow through the TCs are measured internally inside the oil conditioning unit using SKF gear flow monitors. The cooling water flow rate through the EDC is measured internally in the Regloplas P140smart unit.

Pressure sensors, both absolute and gauge, are used in recording static pressures in different sections of the gas stand and the engine. As mentioned earlier, a pressure ring measured the average static pressure across the test section pipe. The location of the different pressure sensors are specified in **Figure 8**. The range of the sensors used and their accuracy are specified in **Table 8**.

Static temperature measurements are done at the inlet and outlet of the TC compressor and the turbine and the EDC in a measuring section. The place where the air/exhaust gas temperatures are below 200°C, PRTs are used in the measurement and in locations where the temperatures are above this, K-type thermocouples of 1.5mm diameter have been used. Except at the inlet of the compressor and the EDC which have two temperature measurement ports, all of the remaining sections have four measurement ports. The lengths of the thermocouples and PRTs used in the compressor and EDC outlet and turbine inlet and outlet sections are the same and are represented in **Figure 5**. Their range and accuracy are specified in **Table 8**.

TC speed is monitored using an eddy current sensor positioned in the compressor housing. By setting up a jumper in a position that corresponds to the number of blades on the compressor wheel, the sensor measures the number of passing blades. The TC speed is derived by correlating the blade setting with the number of passing blades over a given period. The accuracy of the sensor is ±0.5%.

Table 7: Flow meters used, principle, medium and location on the test rig

Measurement fluid type	Purpose or location on the test rig	Flow meter used	Measurement principle
Compressor air flow	Compressor inlet	ABB	Hot film anemometer
Engine air flow	Boost rig outlet	Sierra	Immersible Thermal Mass Flow Meter
Exhaust gas	Turbine outlet	Vcone	Differential pressure
Lubricating oil	TC lubrication system (bespoke unit)	SKF	Gear flow monitors
Cooling water	EDC cooling system (Regloplas P140smart)	Inbuilt	-

Table 8: Sensor types, range and accuracy

Sensor	Range	Accuracy
PRT	-50°C to +200°C	0.3 + 0.005*T
K type TC	-200°C to 1260°C	0.0075*T
Fuel flow	0 to 200 Kg/h	±0.05%
Pressure transducers	-1 barA to 6 barA	0.25%
Turbo speed	0 to 400,000 rpm	0.1%
Exhaust gas mass flow	30 to 300 kg/h 50 to 750 kg/h	±0.5% of the measured value
Air mass flow	0 to 700 kg/h	< 1% of measured value

4. EXAMPLE APPLICATION

The rig was constructed based on the 1D model input of having a 30 litre pulse attenuator to dampen any flow pulsation with a steady mass flow at the turbine outlet. This eventually allowed steady mass flow measurement and hence characterising the TC under steady flow conditions. Following this the EGS was built as discussed in **section** 3. An oversized 2.2 l engine has been chosen in order to provide enough energy to the TC turbine across the entire speed range while accounting for heat loss from the pipe and settling tank. It is important to note that although the engine employs an EGR path, it was kept closed throughout all the tests discussed in this paper.

4.1 DESCRIPTION OF AN EXAMPLE COMPLEX AIR PATH

A complex air path is discussed in this section which uses components from the THOMSON project as a case study to evaluate the test rig. The air path used for the case study consists of a VGT TC, EDC, CAC, LP, HP and mid route EGR and coolers. **Figure 8** shows the three parts of test facility namely: CAHU (boost rig in purple line), engine (blue line), and the gas stand (brown line). The air path consists of a first stage TC compressor and a second stage EDC which could be bypassed if required. The exact layout of these is flexible; one such comparison is made in **section 5.3**.

The engine is supplied with boost air from CAHU and the exhaust gas coming out of the engine goes via the pulse attenuator (bypassed for pulsating/transient tests) before powering the turbine. In the configuration shown in **Figure 8**, an EDC is the second-stage boosting system and thus air flows through the two stages. The air flow rate across the TC compressor and EDC is controlled via the CBPV. The exhaust gas for EGR can be taken from HP, LP and mid routes 1 and 2 as shown in **Figure 8** using manually-actuated poppet valves. Depending on the requirement, individual components can be characterised or could be combined to do the system level mapping. The next section discusses the methodology adopted to perform different tests.

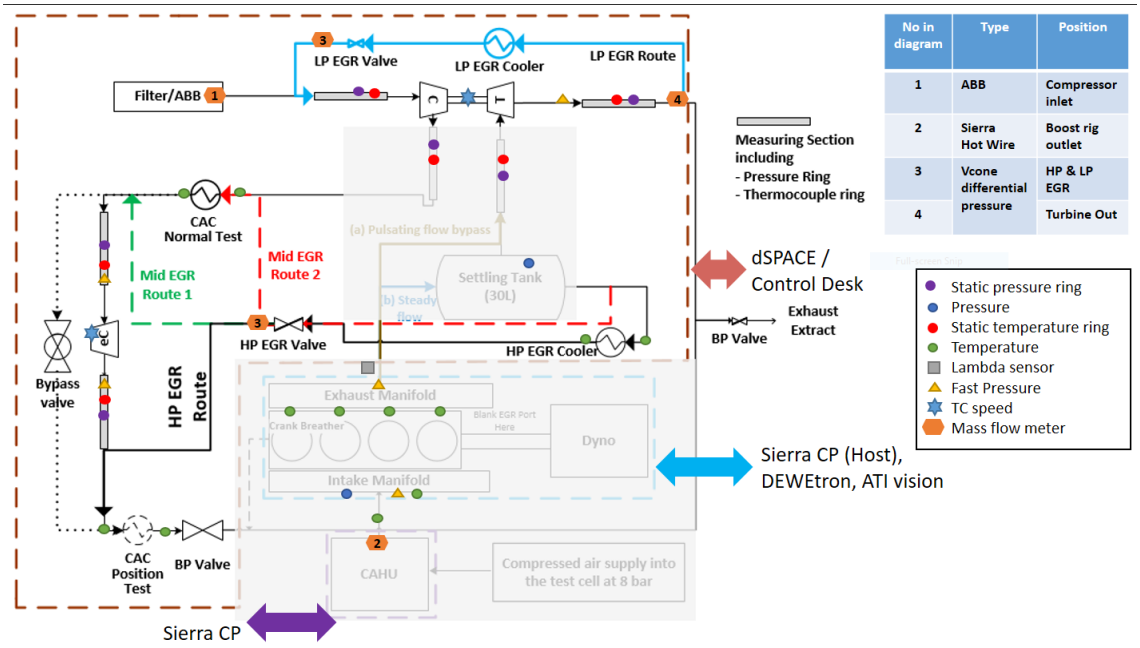

Figure 8: Example flexible air path layouts used in THOMSON project.

4.2 METHODOLOGY FOR DIFFERENT TESTS

4.2.1 TC COMPRESSOR MAPPING METHOD

The compressor is powered by the turbine, driven by the exhaust gases from the engine. The compressor flow is then controlled by the CBPV. For compressor mapping, a number of elements of the prototype air path that are not needed are removed (like the engine EGR valve).

A typical mapping method to get to a single operating point is illustrated in **Figure 9**.

- Starting at point A, reduction in compressor mass flow shifts the operating point to point B
- Adjustments in the turbine power return to point C, which has the same speed as point A

When conducting a complete speed line, the process resembles that shown in **Figure 9**. The compressor operating point was varied from choke to surge for four compressor corrected speeds. The compressor efficiency was calculated based on the SAE recommendations [35]. The process is more onerous than using a conventional steady flow GS, and if only steady flow maps are required this new facility is not the most efficient tool.

Apart from the steady flow mapping setup discussed above compressor mapping can be undertaken under three different configurations to observe the effect of flow unsteadiness:

a) Engine pulsations at the turbine inlet and compressor outlet like a turbocharged engine
b) Engine pulsation only on the turbine side without a settling tank
c) Engine pulsation only on the compressor side connected to the engine intake with a settling tank at the turbine inlet

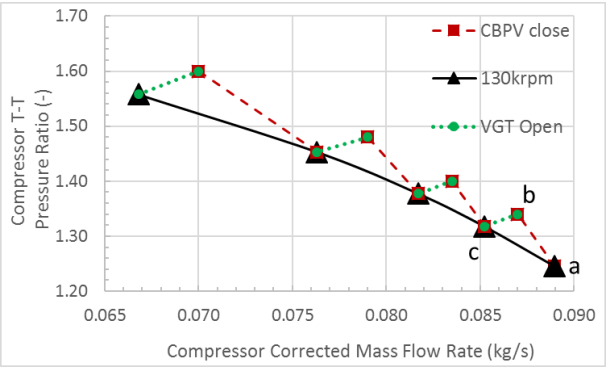

Figure 9: Compressor mapping procedure

An example of steady flow compressor map is shown in section 5.1. In any configuration, different compressor operating conditions are achieved by closing the CBPV or by increasing the flow from the boost rig or the engine speed. Closing the CBPV allows a reduction in mass flow through the compressor. As this mass flow is reduced, typically the TC speed increases as the compressor power absorbed is reduced while the turbine power remains the same. To maintain a constant speed line, the turbine power must be adjusted by either its VGT or waste gate or by reducing the turbine mass flow rate. However, changes in the mass flow rate are coupled to the gas temperature in this facility and therefore care must be taken. turbine inlet temperature (TIT) was kept constant at 823K by varying the intake boost and the throttle signal which is linked to fuel injection in the engine ECU AFR (air-fuel ratio) control.

4.2.2 STEADY FLOW AND LOW FREQUENCY TURBINE MAPPING METHOD

The TC used has a VGT whose position was regulated by an aftermarket VGT regulator. The regulator has a target and an actual position on its display which can be manually varied by the test cell operator. Turbine mapping can be performed under pulsating or steady conditions through the inclusion or bypassing of the settling tank (see **Figure 8**).

The turbine mapping procedure remains similar between steady and unsteady flows although the sensor frequency response requirements are entirely different. The vane angle or the rack position was set to a specific value and the mapping exercise was carried out at 823K TIT. The turbine efficiency was calculated using SAE J1826 [36] recommendations as in equation (1):

$$\eta_t = \frac{\dot{m}_a C_{pa}(T_{02} - T_{01})}{\dot{m}_e C_{pe} T_{03}\left(1 - \left(\frac{1}{(PR_{3-4})^{\frac{(\gamma_{3-4}-1)}{\gamma_{3-4}}}}\right)\right)} \quad (1)$$

The inclusion of the settling tank removes the exhaust pulsations and essentially allows the test rig to behave like a normal steady flow GS. This avoids the difficulties in measuring pulsating flow rates, temperature and pressures. Nevertheless, the thermal and bulk flow transients can still be performed by changing the engine fueling and speed. Turbine mapping is undertaken in much the opposite manner to the compressor mapping where the VGT or closed waste-gate conditions are held constant throughout. To explain this in an example, we move from the highest PR and corrected mass flow rate point P1 in **Figure 10** to the lowest PR and corrected mass flow rate point P5 without changing the VGT position. From point P1, the CBPV is opened and this drops the TC speed. In order to achieve target TC speed and TIT, the boost pressure (CAHU) and engine speed and/or torque (fuel quantity) are reduced. This reduces the PR and mass flow rate across the turbine thus moving to P2. The process is repeated to get the remaining points and all six rack positions were characterised over a range of TC speed.

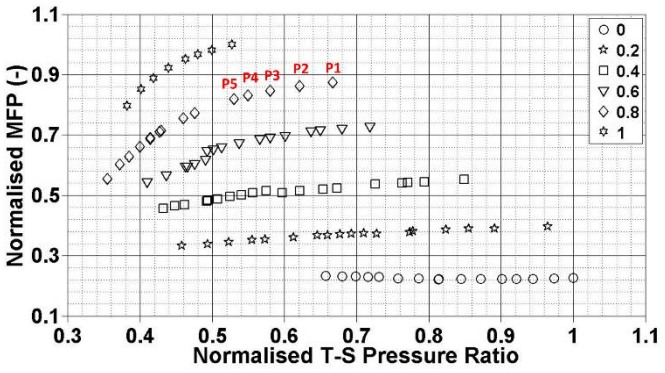

Figure 10: Turbine mapping procedure

4.2.3 ELECTRICALLY DRIVEN COMPRESSOR MAPPING METHOD

This is done essentially on an EDC test stand which is made by isolating certain parts of the system. In its most basic form the EDC is connected to the inlet and outlet measurement sections, upstream mass flow sensor and flows against the CBPV. This layout is shown in **Figure 11**. The EDC is connected to a 48V power supply system and a proportional CAN signal from dSPACE/Control Desk maintains a steady EDC speed even when the CBPV is closed. This makes the mapping process relatively simple. The mass flow rate was varied from choke to surge while giving enough settling time before logging the data. The air filter/ABB assembly can also be replaced by the boost rig to test the EDC with higher than ambient inlet pressure which is more realistic of its operation within the air path.

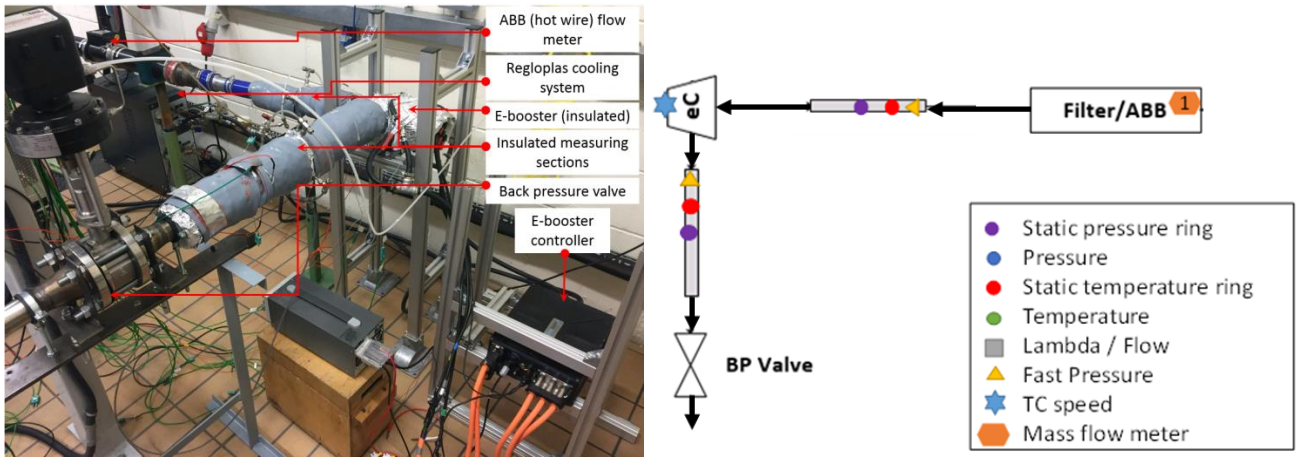

Figure 11: Test rig for characterizing EDC in standalone conditions

4.2.4 TWO-STAGE MAPPING TESTING METHOD

The objective of these tests is to validate the system level model and use it to study the effect of different configurations. The two-stage mapping essentially uses the configuration of the complete test rig already shown in **Figure 1**. This configuration involves a first-stage TC compressor and a second stage EDC with the CBPV positioned after the EDC. The target or the test points were supplied by a validated 1D model provided by the project partners. The test point discussed here comes from a low engine speed full load condition where the EDC operates close to its full potential.

The test was done by running the engine at a certain speed and load with the boost rig supplying enough mass flows and boost pressure. The TC speed was matched by adjusting the above parameters along with the VGT vane angle. The EDC speed was increased in 5000 rpm steps as the TC speed increases. The CBPV is closed gradually along with the above steps. The air mass flow rate through the TC compressor and the EDC are the same. When the target TC speed, EDC speed and air mass flow was achieved the entire system is left to reach a thermally steady condition before logging the data.

The inlet pressure of the EDC is changed by running the TC at different speeds, and mapping is performed at different upstream conditions characterizing the EDC by varying the CBPV position at different EDC speeds. The resulting data could be used in 1D modeling studies and also to analyse the influence of the first stage on the EDC performance.

4.2.5 CAC POSITION TEST METHOD

The intercooler for required cooling the compressed air from the TC compressor or the EDC compressor could be positioned either between the two stages or after the two stages. To compare the effect of its position, the CAC was moved to after the second stage. Identical test points were compared with tests having the CAC between the two stages. The operating procedure remains the same as described in **section 4.2.4**. The TC and EDC were run at physically the same condition (in terms of VGT position, PR, mass flow rate and TC speed) in order to observe the thermal effect.

5. RESULTS AND DISCUSSION

The results of the component and system level test performed on the EGS are discussed in this section. An example is presented for each test method explained in section 4.2. The facility is not hardware specific and could be used for simple to complex air paths.

5.1 COMPONENT LEVEL TESTING

Example dataset representing the characteristics for a TC compressor, a turbine (VGT) and an EDC is presented. An example compressor map generated with steady flow on both turbine and compressor side (as in a GS) is presented. **Figure 12** and **Figure 13** shows the comparison of steady flow compressor map obtained from the EGS and conventional GS (obtained on a conventional turbocharger gas stand rig). The compressor PR on the EGS is higher (**Figure 12**) at lower mass flow rate than the conventional GS and it is lower at high mass flow rates. This could be due to the change in the pipe sizes and bends at the compressor inlet and outlet. The change in PR seems to have a similar effect on the compressor efficiency as shown in **Figure 13**. This is not entirely due to the change in PR but also with the change in the TIT (823K on the EGS and 873K on the GS). This is in line with the previous study performed at two different TITs (600K and 830K) where the 600K case had a higher efficiency [24].

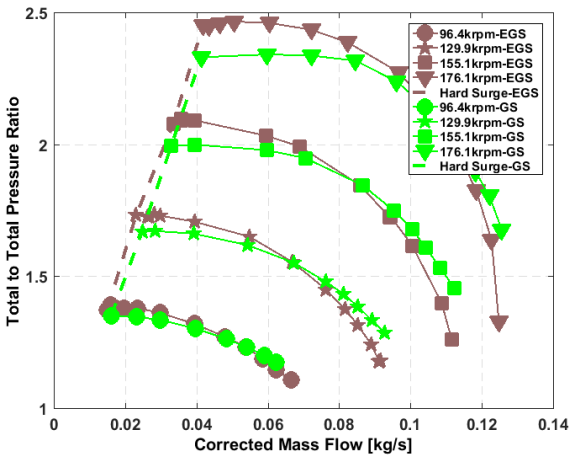

Figure 12: Steady flow compressor map obtained from engine gas stand with a settling tank and conventional turbocharger gas stand

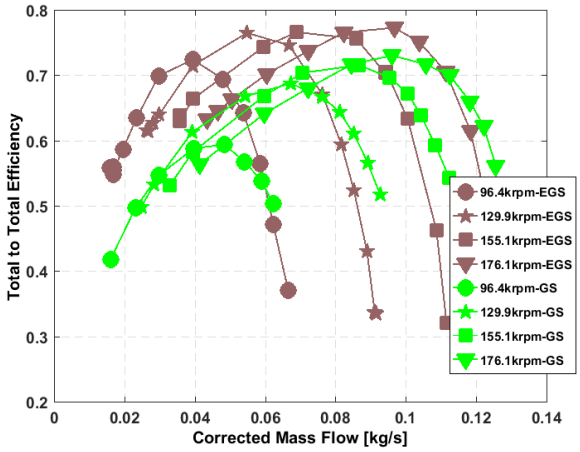

Figure 13: Steady flow compressor efficiency obtained from engine gas stand with a settling tank and conventional turbocharger gas stand

An example steady flow turbine characteristics map obtained on the EGS while using the settling tank (to steady the flow) is compared with the one obtained on the conventional turbocharger GS as shown in **Figure 14** and **Figure 15**. There is good agreement seen in terms of the turbine mass flow parameter (MFP) and total-to-static (T-S) PR across the turbine for all the rack positions except at low PRs where there is a small difference (**Figure 14**). The turbine efficiency obtained on the EGS is lower compared to that obtained on the GS. This is mostly due to the difference in TIT (823K on EGS Vs 873K on the conventional GS) and the associated heat transfer characteristics. This is in line with results from other researchers [37].

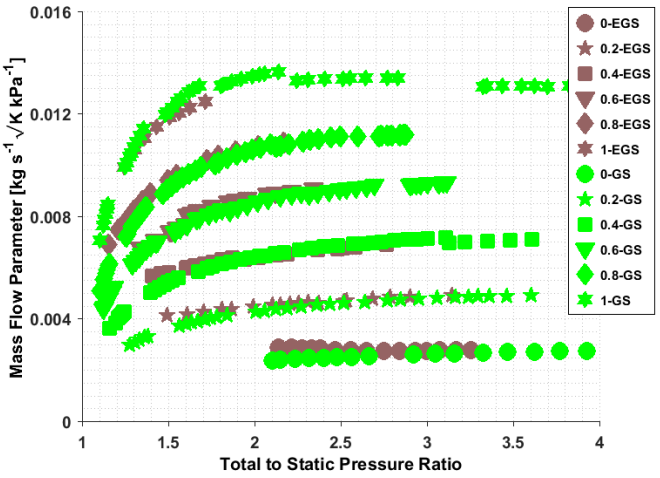

Figure 14: Steady flow Turbine map obtained from engine gas stand with a settling tank and conventional turbocharger gas stand

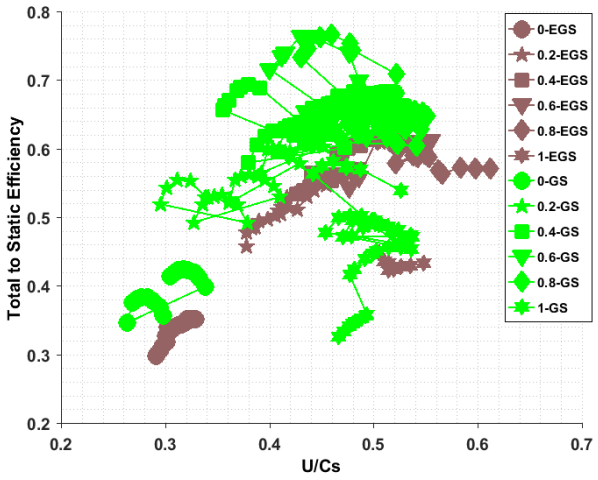

Figure 15: Turbine efficiency map for different VNT rack positions obtained from engine gas stand with a settling tank and conventional turbocharger gas stand

A comparison of an example map obtained from the EDC setup and that from the manufacturer is shown in **Figure 16** and **Figure 17**. There seems to be significant shift in the location of surge and the shape of the line going into surge. On the test conducted on the facility (EGS) it is flatter whereas the one from the manufacturer has a dip in PR before the surge. The compressor efficiency is sensitive to PR. Again the difference in pipework could account for this change in surge behavior and could also cause a difference in compressor efficiency [38].

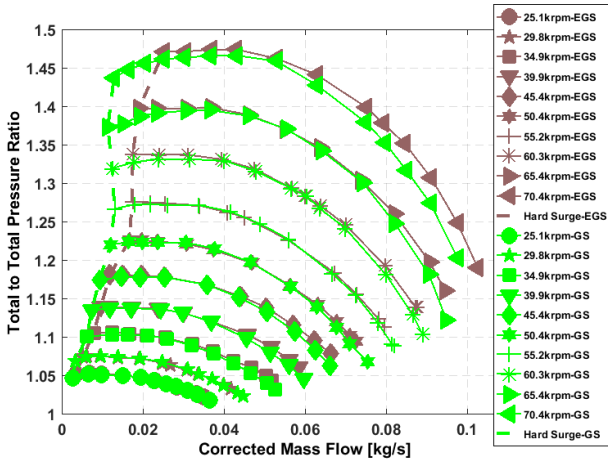

Figure 16: Steady flow EDC map

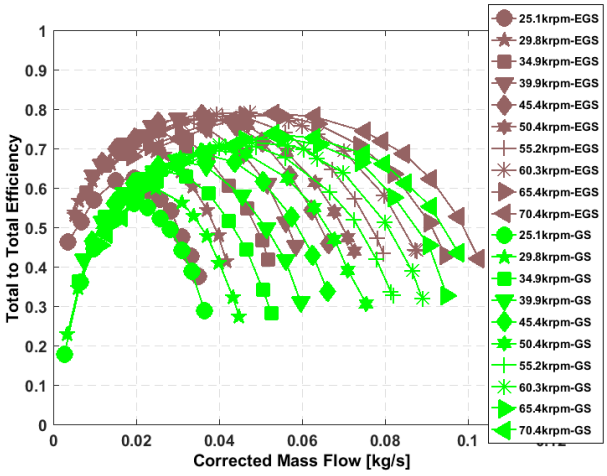

Figure 17: Steady flow EDC efficiency

5.2 2-STAGE BOOSTING SYSTEM

Example test points from a system test on the THOMSON layout are discussed. The test points from a 1.6 l downsized diesel used in the THOMSON project are taken at the following engine speeds where the EDC operates close to its full potential: 1000 rpm and 1500 rpm. An example data set of the EDC and TC compressor operating points from the EGS for a 2-stage boosting system is shown in **Figure 18** and **Figure 19** respectively. To negotiate the effect of temperature and pressure, mass flow terms have been corrected for temperature and pressure. It could be observed from the figures there is a good match between the 1D modeling and the test results in the above configuration. The EGS can thus be used for system level tests with a good accuracy and in this case replicates the THOMSON layout.

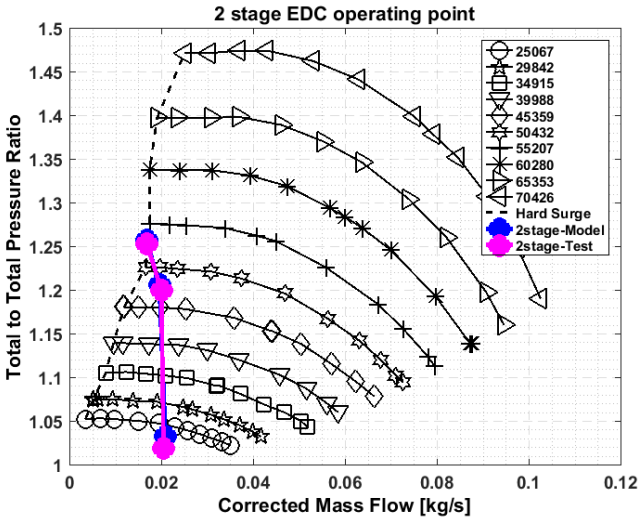

Figure 18: EDC operating point in EGS under steady flow and 1D engine model in 2-stage configuration

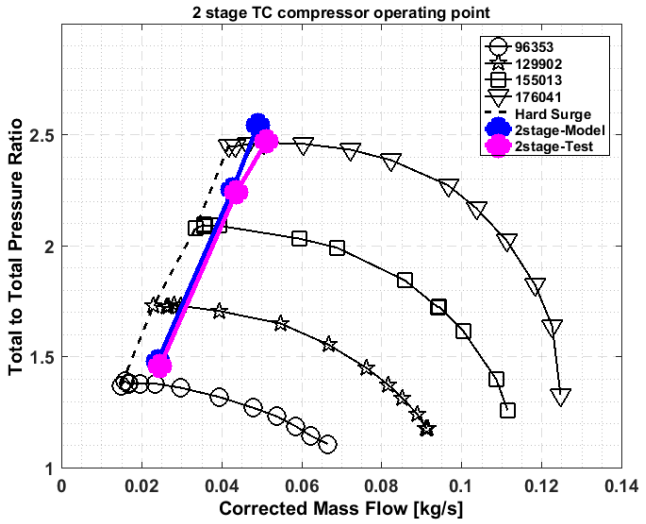

Figure 19: Compressor operating point in EGS under steady flow and 1D engine model in 2 stage configuration

5.3 INTERCOOLER POSITIONING

The air path considered in this case study is flexible. Positioning the CAC hardware is one of the key decisions to be made. Thus the intercooler was positioned between the two boosting systems (1st-CAC in **Figure 20** to **Figure 22**) and after the two boosting stages (2nd-CAC in **Figure 20** to **Figure 22**). Similar test conditions were maintained when testing it at two locations. For example, the TC and the EDC speeds were similar as shown in **Figure 20**. Identical air mass flow rate was maintained in the two cases across the EDC and the TC compressor as shown in **Figure 21**. The PR across the EDC dropped marginally when the intercooler was positioned after the EDC (**Figure 21**) mainly due to higher EDC inlet and outlet temperature reducing the outlet pressure.

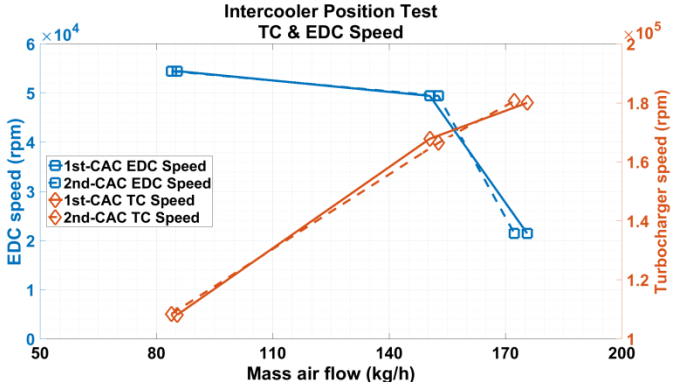

Figure 20: Similar TC and EDC speed maintained in the two set of tests

Another important observation made was that the EDC acts as a sink for heat rejection when the TC operates at high speed. This could be seen from the lower EDC outlet temperature being lower compared to the inlet temperature in **Figure 22**. This significant cooling effect of the EDC is not typically modelled and the test data would be used to improve and calibrate the air path of the 1D model. Consequently the 1D model will be used to observe the effect of positioning the intercooler on the engine performance (this is outside the scope of this paper).

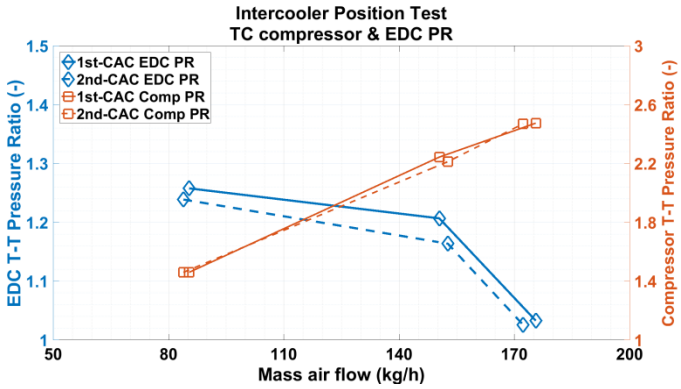

Figure 21: Identical mass flow rate but different EDC PR observed

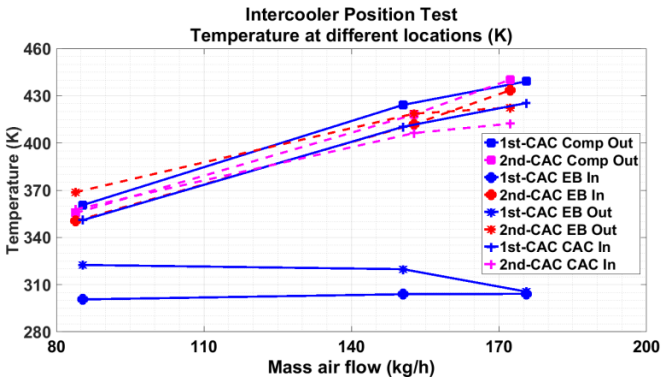

Figure 22: Temperature at different location in the 2-stage system test

6. CONCLUSION

A new test facility has been constructed at the University of Bath with the intention to undertake steady flow and transient characterization for a complex air path system and investigate potential future system layouts and control strategies. The test facility is flexible and allows for the study of individual components and full systems. The facility also allows for the replication of realistic, on-engine boundary conditions but also separating out physical phenomena to promote the scientific study of the system behavior.

The test facility is constructed around a 2.2 l diesel engine with new support systems constructed or adapted specifically to suit the component tested. These include a boost emulation rig, a pulse attenuator, oil and water conditioning systems and gas stand-like measurement equipment. The complex rig also has a bespoke control hardware system to support it.

Individual aspects of the test facility have been commissioned and have produced results using specific hardware. At the component level these include compressor,

turbine and EDC mapping approaches as well as investigation of a 2-stage boosting system, the effect of positioning the CAC and initial T_4 studies. The next steps will be to use the hardware to perform EGR and transient studies.

ACKNOWLEDGMENTS

This work was conducted with funding from the THOMSON project which has received funding from the European Union's Horizon 2020 Programme for research, technological development and demonstration under Agreement no. 724037.

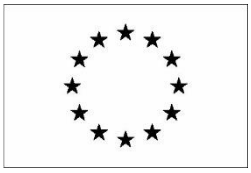

REFERENCES

[1] V. Das, S. Padmanaban, K. Venkitusamy, R. Selvamuthukumaran, F. Blaabjerg, and P. Siano, "Recent advances and challenges of fuel cell based power system architectures and control – A review," *Renewable and Sustainable Energy Reviews*, vol. 73, no. January, pp. 10–18, 2017.

[2] O. Z. Sharaf and M. F. Orhan, "An overview of fuel cell technology: Fundamentals and applications," *Renewable and Sustainable Energy Reviews*, vol. 32, pp. 810–853, 2014.

[3] S. Ichikawa *et al.*, "Development of New Plug-In Hybrid System for Compact-Class Vehicle," *SAE International Journal of Alternative Powertrains*, vol. 6, no. 1, pp. 2017-01-1163, 2017.

[4] W. Eckerle, V. Sujan, and G. Salemme, "Future Challenges for Engine Manufacturers in View of Future Emissions Legislation," in *SAE Technical Paper*, 2017, vol. 2017-01-19.

[5] A. M. I. Mamat, A. Romagnoli, and R. F. Martinez-Botas, "Characterisation of a Low Pressure Turbine for Turbocompounding Applications in a Heavily Downsized Mild-hybrid Gasoline Engine," *Energy*, vol. 64, pp. 3–16, 2014.

[6] D. Koeberlein, "Cummins Supertruck Program Technology and System Level Demonstration of Highly Efficient and Clean, Diesel Powered Class 8 Trucks," in *2015 DOE Hydrogen and Fuel Cells Program and Vehicle Technologies Office Annual Merit Review and Peer Evaluation Meeting*, 2015, p. 30.

[7] M. Bassett *et al.*, "Heavily Downsized Gasoline Demonstrator," *SAE International Journal of Engines*, vol. 9, no. 2, pp. 2016-01–0663, 2016.

[8] R. Salehi, J. Martz, A. Stefanopoulou, T. Hansen, and A. Haughton, "Comparison of High- and Low-Pressure Electric Supercharging of a HDD Engine : Steady State and Dynamic Air-Path Considerations," in *SAE Technical Paper*, 2016, no. 2016-01-1035.

[9] A. J. Feneley, A. Pesiridis, and A. M. Andwari, "Variable Geometry Turbocharger Technologies for Exhaust Energy Recovery and Boosting-A Review," *Renewable and Sustainable Energy Reviews*, vol. 71, pp. 959–975, 2017.

[10] M. Kobayashi *et al.*, "Effective BSFC and NOx Reduction on Super Clean Diesel of Heavy Duty Diesel Engine by High Boosting and High EGR Rate," in *SAE Technical Paper*, 2011, no. 2011-1–369.

[11] Y. Park and C. Bae, "Experimental study on the effects of high/low pressure EGR proportion in a passenger car diesel engine," *Applied Energy*, vol. 133, pp. 308–316, 2014.

[12] M. S. Khalef, A. Soba, and J. Korsgren, "Study of EGR and Turbocharger Combinations and Their Influence on Diesel Engine's Efficiency and Emissions," *SAE Technical Paper*, no. 2016-1–676, 2016.

[13] F. Hellstrom, U. Renberg, F. Westin, and L. Fuchs, "Predictions of the Performance of a Radial Turbine with Different Modeling Approaches: Comparison of the Results from 1-D and 3-D CFD," in *SAE Technical Paper 2010-01-1223*, 2010.

[14] C. D. Copeland, R. Martinez-Botas, and M. Seiler, "Comparison Between Steady and Unsteady Double-Entry Turbine Performance Using the Quasi-Steady Assumption," *ASME. Turbo Expo: Power for Land, Sea, and Air, Volume 7: Turbomachinery, Parts A and B*, vol. 7, pp. 1203–1212, 2009.

[15] J. Galindo, H. Climent, C. Guardiola, and A. Tiseira, "On the Effect of Pulsating Flow on Surge Margin of Small Centrifugal Compressors for Automotive Engines," *Experimental Thermal and Fluid Science*, vol. 33, no. 8, pp. 1163–1171, 2009.

[16] F. J. Wallace, J. M. Adgey, and G. P. Blair, "Performance of Inward Radial Flow Turbines Under Non-steady Flow Conditions," *Proceedings of the Institution of Mechanical Engineers*, vol. 185, no. 1, pp. 1091–1105, 1970.

[17] J. R. Serrano, F. J. Arnau, P. Fajardo, M. A. Reyes-Belmonte, and F. Vidal, "Contribution to the Modeling and Understanding of Cold Pulsating Flow Influence in the Efficiency of Small Radial Turbines for Turbochargers," *ASME. J. Eng. Gas Turbines Power*,

vol. 134, no. 10, pp. 102701–11, 2012.

[18] S. Szymko, R. F. Martinez-Botas, and K. R. Pullen, "Experimental evalation of turbocharger turbine performance under pulsating flow conditions," *ASME Turbo Expo 2005: Power for Land, Sea, and Air*, vol. 6, pp. 1447–1457, 2005.

[19] M. Capobianco and S. Marelli, "Waste-Gate Turbocharging Control in Automotive SI Engines : Effect on Steady and Unsteady Turbine Performance," *SAE Technical Paper 2007-01-3543*, 2007.

[20] C. Copeland, G. Capon, D. Witt, and S. Akehurst, "A Novel Pulse Generator for Turbocharger Gas Stand Application," 83605987, 2015.

[21] V. De Bellis, S. Marelli, F. Bozza, and M. Capobianco, "1D simulation and experimental analysis of a turbocharger turbine for automotive engines under steady and unsteady flow conditions," *Energy Procedia*, vol. 45, pp. 909–918, 2014.

[22] R. Bontempo, M. Cardone, M. Manna, and G. Vorraro, "Highly flexible hot gas generation system for turbocharger testing," *Energy Procedia*, vol. 45, pp. 1116–1125, 2014.

[23] J. M. Luján, V. Bermúdez, J. R. Serrano, and C. Cervelló, "Test Bench for Turbocharger Groups Characterization," *SAE Technical Paper 2002-01-0163*, 2002.

[24] C. Avola, P. Dimitriou, R. Burke, and C. Copeland, "Preliminary DoE Analysis and Control of Mapping Procedure for a Turbocharger on an Engine Gas-Stand," in *ASME. Turbo Expo: Power for Land, Sea, and Air, Volume 8: Microturbines, Turbochargers and Small Turbomachines; Steam Turbines ():V008T23A008*, 2016, pp. 1–14.

[25] C. Avola, C. Copeland, T. Duda, and R. Burke, "Compressor Surge for Fully and Semi Fluctuating Flows in Automtoive Turbochargers," in *Proceedings of the 1st Global Power and Propulsion Forum*, 2017, pp. 1–9.

[26] C. Avola, C. Copeland, T. Duda, R. Burke, S. Akehurst, and C. Brace, "Review of Turbocharger Mapping and 1D Modelling Inaccuracies with Specific Focus on Two-Stag Systems," in *SAE International*, 2015.

[27] C. Avola, C. Copeland, R. Burke, and C. Brace, "Numerical Investigation of Two-Stage Turbocharging Systems Performance," in *ASME 2016 Internal Combustion Engine Division Fall Technical Conference (): V001T07A007*, 2016, pp. 1–9.

[28] C. Avola, C. D. Copeland, R. D. Burke, and C. J. Brace, "Effect of inter-stage phenomena on the performance prediction of two-stage turbocharging systems," *Energy*, vol. 134, pp. 743–756, 2017.

[29] S. Ye, "Oxidation Catalyst Studies on a Diesel Engine," Thesis (Doctor of Philosophy (PhD)), University of Bath, Bath, United Kingdom, 2010.

[30] G. Mahadevan and S. Subramanian, "Experimental Investigation of Cold Start Emission using Dynamic Catalytic Converter with Pre-Catalyst and Hot Air Injector on a Multi Cylinder Spark Ignition Engine," in *SAE Technical Paper*, 2017, no. 2017-01-2367.

[31] J. Pihl *et al.*, "Development of a Cold Start Fuel Penalty Metric for Evaluating the Impact of Fuel Composition Changes on SI Engine Emissions Control," in *SAE Technical Paper*, 2018, no. 2018-01-1264, pp. 1–8.

[32] R. Vijayakumar, "Turbo-discharging Turbocharged Internal Combustion Engines," Loughborough University, 2016.

[33] B. Hu, S. Akehurst, C. Brace, C. Copeland, and J. Turner, "1-D Simulation Study of Divided Exhaust Period for a Highly Downsized Turbocharged SI Engine - Scavenge Valve Optimization," *SAE International Journal of Engines*, vol. 7, no. 3, pp. 1443–1452, 2014.

[34] K. Zhang, "Air Charge System Emulation for Diesel Engine," 2010.

[35] SAE_J1723, "Supercharger testing standard," in *Surface Vehicle Standard*, 1995, pp. 1–9.

[36] SAE_J1826, "TURBOCHARGER GAS STAND TEST CODE," in *SAE International*, 1995, pp. 1–12.

[37] J. R. Serrano, C. Guardiola, V. Dolz, A. Tiseira, and C. Cervelló, "Experimental Study of the Turbine Inlet Gas Temperature Influence on Turbocharger Performance," in *SAE Technical Paper*, 2007.

[38] J. Galindo, A. Tiseira, R. Navarro, D. Tarí, and C. M. Meano, "Effect of the Inlet Geometry on Performance, Surge margin and Noise Emission of an Automotive Turbocharger Compressor," *Applied Thermal Engineering*, vol. 110, pp. 875–882, 2017.